Material Analysis by the Nuclear Backscattering Method Using Cyclotron

AUTHOR(S):

Hayashi, Yasuaki; Igaki, Takao; Takekoshi, Hidekuni

Bull. Inst. Chem. Res., Kyoto Univ., Vol. 56, No. 1, 1978

Material Analysis by the Nuclear Backscattering Method Using Cyclotron

Yasuaki HAYASHI, Takao IGAKI, and Hidekuni TAKEKOSHI*

Received January 9, 1978

Organic matters have been analyzed with nuclear backscattering method using the Kyoto University cyclotron. The energies of the beams used in these experiments are higher than those commonly used in the nuclear backscattering analysis. About the local distribution of light elements in the samples, the resolution of about 1 micron at the depth of 20 micron is obtained. The elemental ratio can be decided precisely for the sample of 5×10^{16} molecules/cm^2.

I. INTRODUCTION

Nuclear backscattering analysis is a useful method to determine composition variation or impurity distribution as a function of depth below the surface of a sample.[1~3] In this method, the sample to be analyzed is bombarded with a monoenergetic beam of light ions and the energy of particles elastically scattered backward is measured. From the energy spectrum the information on the elemental composition near the surface can be obtained.

The principle of this technique is illustrated in Fig. 1. The kinematic factor, K, is the ratio of the projectile energies after (E) and before (E_0) collision at the surface, *i.e.*,

$$K(M, m, \theta) \equiv \frac{E}{E_0} \tag{1}$$

$$= \left\{ \frac{M\cos\theta}{M+m} + \left[\left(\frac{M\cos\theta}{M+m} \right)^2 + \frac{M-m}{M+m} \right]^{1/2} \right\}^2, \tag{2}$$

where m is the mass of the projectile, M is that of the element to be analyzed, and θ is the scattering angle. When a particle is scattered at the depth t in the target, it loses the energy during the passage through the target material. In case the incident angle of the projectile is θ_1 with respect to the normal of the target, the energy E' of the projectile at the depth t just before the scattering is given by

$$E' = E_0 - \int_0^{\frac{t}{\cos\theta_1}} \frac{\mathrm{d}E}{\mathrm{d}X}\mathrm{d}X. \tag{3}$$

After scattering, the particle will also lose its energy in the target, and it will have energy E_1 when emerging from the target with the angle θ_2 to the normal of the target, *i.e.*,

$$E_1 = K(M, m, \theta)E' - \int_0^{\frac{t}{\cos\theta_2}} \frac{\mathrm{d}E}{\mathrm{d}X}\mathrm{d}X, \tag{4}$$

where the scattering angle θ is given by

* 林　康明，伊垣隆夫，竹腰秀邦：Nuclear Science Research Facility, Institute for Chemical Research, Kyoto University, Kyoto.

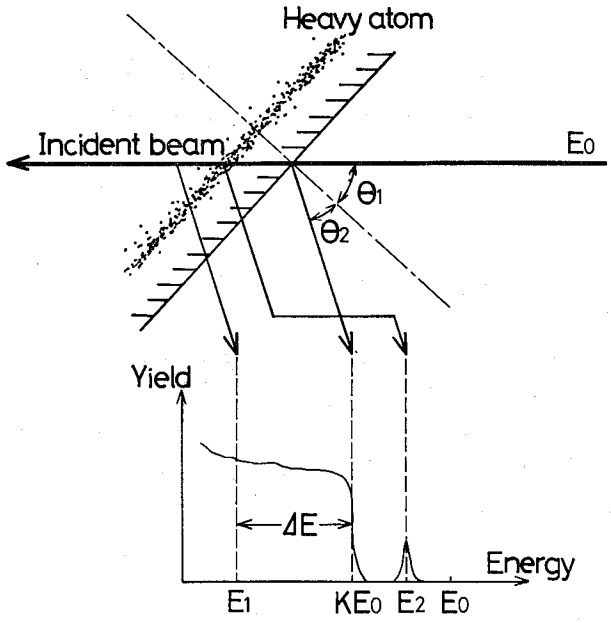

Fig. 1. Principle of nuclear backscattering analysis.

$$\theta=180°-\theta_1-\theta_2. \tag{5}$$

The energy difference, ΔE, between the particle scattered from the atoms on the surface and that scattered from the atoms at depth t is given

$$\Delta E=KE_0-E_1. \tag{6}$$

From equations (3)$\sim$(6), ΔE becomes

$$\Delta E=K\int_0^{\frac{t}{\cos\theta_1}}\frac{dE}{dX}dX+\int_0^{\frac{t}{\cos\theta_2}}\frac{dE}{dX}dX. \tag{7}$$

In equation (7), the kinematic factor K depends on the mass of the target atom to be analyzed and two integrals are functions of the depth of that atom's location. The data of the stopping power, dE/dX, in these integrals is available from the current compilations.[4] Therefore, one can calculate t from equation (7) using the measured value of ΔE. Because the energy loss process is stochastic phenomena, the variance of $\int_0^{\frac{t}{\cos\theta}}\frac{dE}{dX}dX$ must be considered. If the location of the atom to be analyzed is deep, this variance becomes larger and the depth cannot be determined strictly.[5]

The backscattering yield η is directly connected to the quantitative analysis.[1] η depends on the total number of projectiles, n, incident on the target, the average differential scattering cross section, σ, the solid angle of the detecting system, Ω, and the total number of target atoms, N, *i.e.*,

$$\eta=n\sigma\Omega N. \tag{8}$$

The average differential scattering cross section, σ, taken over a finite solid angle, Ω, spanned by the detector, is defined as

$$\sigma=(1/\Omega)\int(d\sigma/d\Omega)d\Omega. \tag{9}$$

The differential scattering cross section, $d\sigma/d\Omega$, deviates significantly from the Rutherford formula for high energy protons and alpha ions in this case because the nuclear force interaction becomes dominant.

The energies of projectile ions commonly used in the nuclear backscattering analysis are under the Coulomb barrier of the nuclear interactions, *i.e.*, the energy of proton ion is below 3 MeV and that of helium ion is below 5 MeV. Using the beams of these energies one can analyze the sample to the depth of a few micron with the position sensitivity of the order of 100 angstrom. But where the depth is more than a few micron, it is necessary to use more energetic ions than above mentioned.

We have tried to analyze the composition of light elements such as carbon, nitrogen and oxygen in the deeper region of the sample by the 6.9 MeV proton beam and 27.6 MeV alpha beam accelerated by the cyclotron of Kyoto University.

II. EXPERIMENTAL

1. Scattering Chamber

Figure 2 shows a view of the chamber of 50 cm in diameter and 30 cm in length used for routine nuclear backscattering analysis and also for nuclear physics experiments. The chamber is a cylindrical shape. The beam enters into the chamber through the beam tube connected to the cylindrical wall of the chamber. Also to the opposite side of the cylindrical wall the beam tube is connected. The beam having

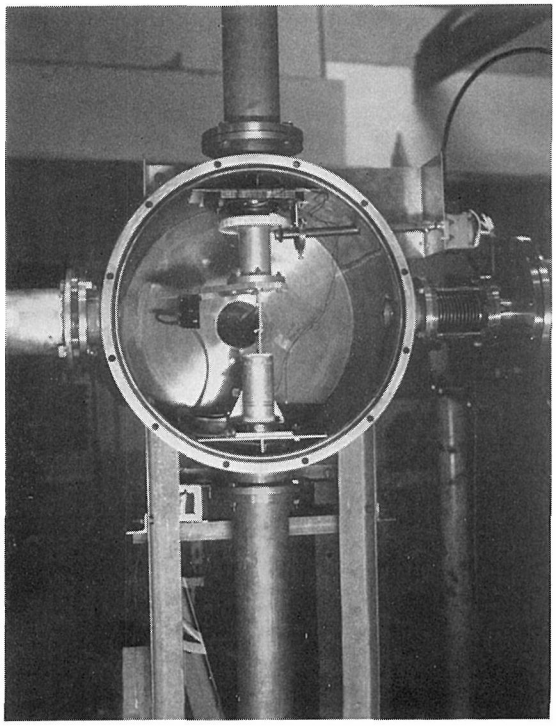

Fig. 2. A complete view of the scattering chamber used for a backscattering analysis.

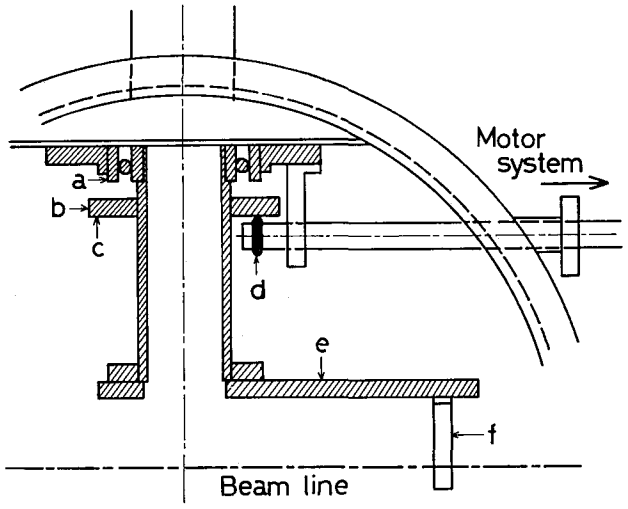

Fig. 3. Schematic diagram of turn table. a) Ball bearing b) Degree scale. c) Turning plate. d) Rubber wheal. e) Detector bed. f) Detector supporter.

passed through the target on the sample holder is transported to a beam catcher which is completely insulated.

Three windows are equipped to the wall of the plane sides of the chamber. The upper two allow observation of the interior, and the lowest allows transmitting of the electricity. To the other side of the chamber a large thin aluminium plate is flanged. Gamma-rays and *X*-rays from the target are detected with the detector placed outside of the chamber through this aluminum plate.

For backscattering analysis of many samples without breaking the vacuum, the target holder should contain as many samples as possible.[6] The samples are fitted to a 40 cm long aluminum frame of the holder, which can slide up and down, and may be changed by a motor system operated in the counting room. The holder can rotate through its axis for changing the glancing angle of the incident beam to the target.

A detector for scattered particles is hanged under a proper position of a turn table to yield a moderate counting rate. The turn table also can be rotated semicirculary by a motor system operated in the counting room. (see Fig. 3)

2. Target

To apply this technique especially to the analysis of the elements in organisms, we prepared the targets of organic matters.

For the depth resolution measurement the targets of "sandwiches" of a golden layer put between two mylar foils of various thicknesses were made. Gold was evaporated on one of the mylar foil, and the thickness of the golden layer was determined by weighting the foil before and after the evaporation.

To get the sensitivity of elemental analysis of this technique, the samples of trace of organic matter spread on a thin copper foil was prepared. The amount of the organic matter was determined by weighting the solution of this matter before spreading and drying.

3. Beam and detector

The bombarding particles used are 6.9 MeV protons and 27.6 MeV alpha particles. Beams are collimated by diaphragms and the cross section of proton beam at the target is 2^{mm} wide, 4^{mm} high, and that of alpha beam is 4^{mm} wide, 6^{mm} high. The beam currents used in the various experiments range from some nanoamperes to 50 nanoamperes.

A silicon surface barrier detector from ORTEC of 14.6 keV energy resolution and 500-microns depletion depth is used. The detector collimated by a diaphragm of 5^{mm} diameter aperture is placed 150^{mm} apart from the target.

III. RESULT AND DISCUSSION

Figure 4 shows a spectrum of scattered particles from the proton bombardment observed at 120°. The glancing angle of the incident beams are usually 90° with respect to the target plane. The target is a "sandwich" of a 700 Å golden layer put between 7 micron mylar and 12 micron mylar foils. A large hill shows the elastic scattering of protons from the carbon atoms in the mylar foils, and a dip at the top of the hill is due to the absence of carbon atoms. Here occupy the golden atoms, and the peak of protons elastically scattered from the golden atoms is seen in the higher energy region. Also a small hill of protons elastically scattered from the oxygen atoms in the mylar foil is seen adjacent the higher energy portion of the carbon hill. On the oxygen hill we can also see a small dip due to the absence of oxygen atoms. It needs only a few minutes to get this spectrum when the beam currents is 50 nanoamperes.

Figures 5, 6, and 7 show spectra of the elastically scattered protons observed at 150°, 120°, and 105° respectively. The target is a "sandwich" of a 2000 Å golden layer put between 24 micron and 12 micron mylars. Comparing these figures, one can

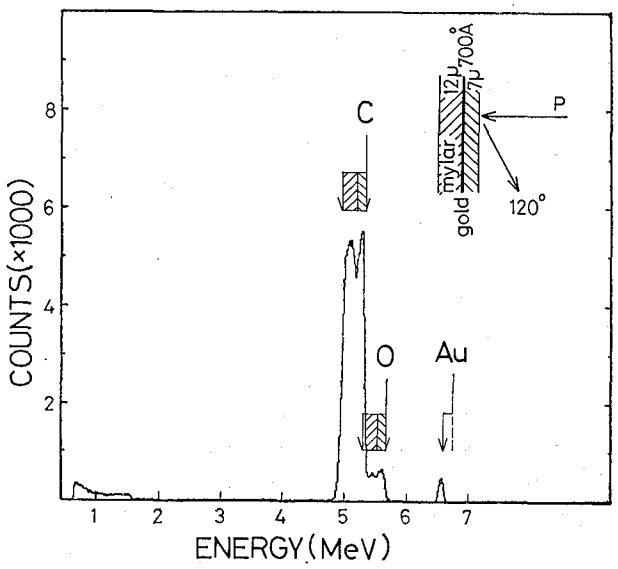

Fig. 4. 6.9 MeV proton backscattering spectrum observed at 120° from a 12 μ mylar-700 Å gold-7μ mylar "sandwich" target.

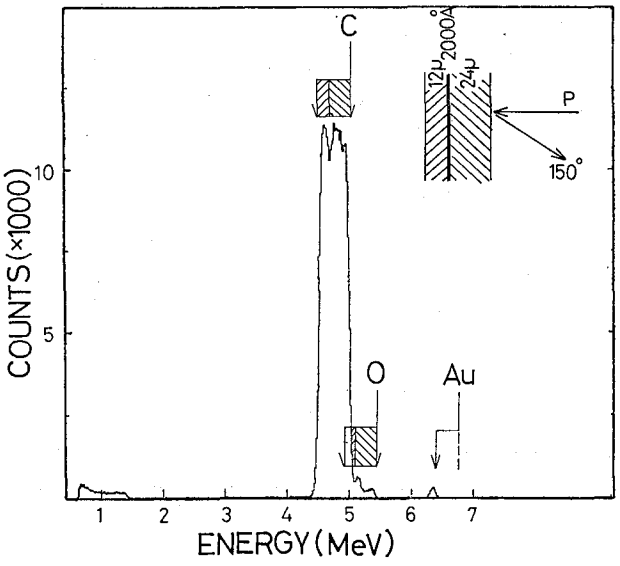

Fig. 5. 6.9 MeV proton backscattering spectrum observed at 150° from a 12 μ mylar-2000 Å gold-24 μ mylar "sandwich" target.

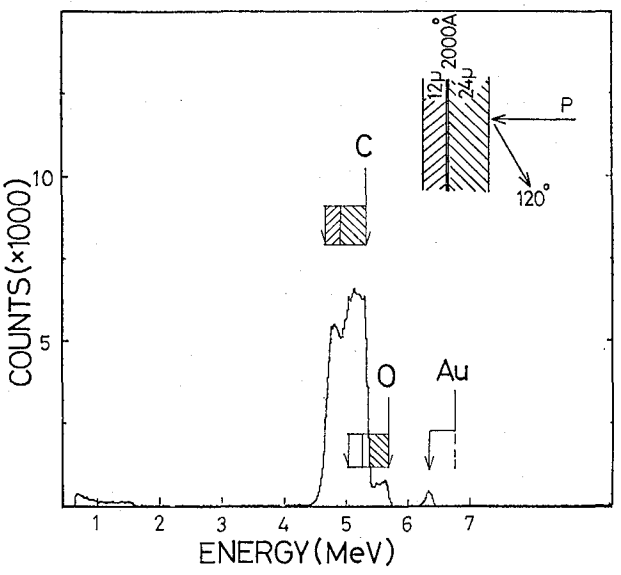

Fig. 6. At 120°. The other conditions are the same as that of Fig. 5.

distinguish the dip at the hill more clearly at 120° scattering than at 150° scattering. This results from the fact that the protons lose more energy at 120° scattering than at 150° scattering. Although protons lose more energy at 105° scattering than at 120° or 150° scattering, the dip on the hill can no more be distinguished. The reason is that the energy straggling of the scattered protons becomes larger with increasing of the energy loss.[5]

Figures 8 and 9 show the spectra of the elastically scattered 6.9 MeV proton and 27.6 MeV alpha particles observed at 150° respectively. In both measurements

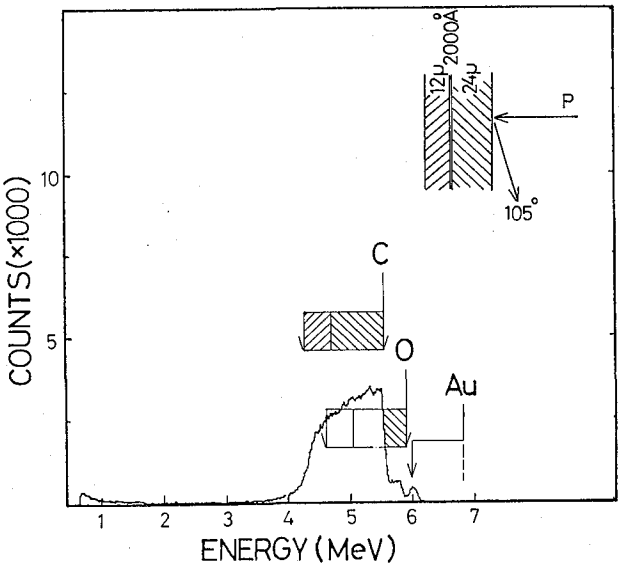

Fig. 7. At 105°. The other conditions are the same as that of Fig. 5.

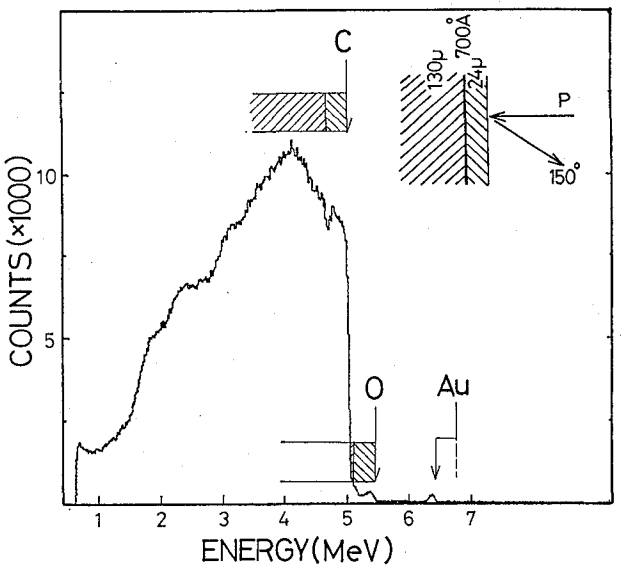

Fig. 8. 6.9 MeV proton backscattering spectrum observed at 150° from a 130 μ mylar-700 Å gold-24 μ mylar "sandwich" target.

the target is the same a "sandwich" of a 700 Å golden layer put between 24 micron and 130 micron mylar foils. In the case of the alpha bombardment the energy straggling of the alpha particles become too large to distinguish a dip on the hill.

Figure 10 shows a spectrum of the scattered particles observed at 150° when proton bombarded a target of organic matter, which is ammonium citrate, $C_6H_5O_7(NH_4)_3$, of 50 μg weight, spread out on a copper foil in area of 2 cm^2. In the spectrum we can see three peaks of carbon, nitrogen and oxygen atoms. The heights of each peak don't correspond to the elemental ratio of each atom in ammonium citrate molecule, because

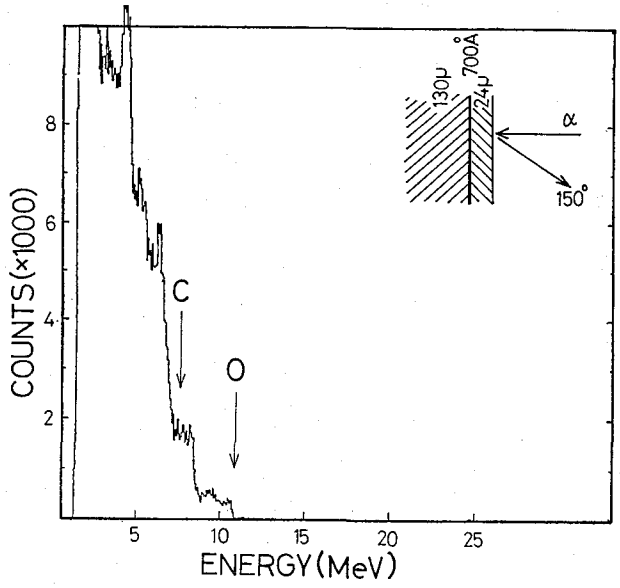

Fig. 9. 27.6 MeV alpha backscattering spectrum observed at 150° from the same target with that of Fig. 8.

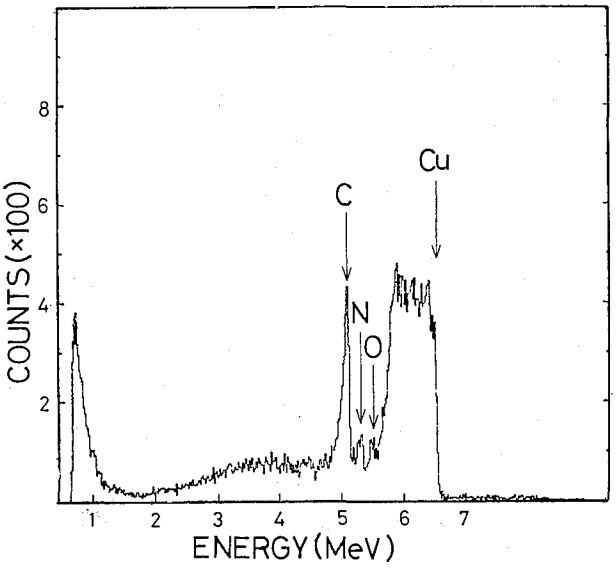

Fig. 10. 6.9 MeV proton backscattering spectrum observed at 150° from ammonium citrate of 50 g weight, 2 cm² area on a copper foil.

the cross sections of the elastic scattering of these three atoms are quite different to one another.

Figure 11 shows the spectrum from the proton bombardment on a target of a cherry leaf. The condition of the bombardment is the same as that of Fig. 11. We can see a dip just below the upper edge in the carbon hill and a peak at the upper edge in the oxygen hill. This peak corresponds to the location of the dip in the carbon hill. This

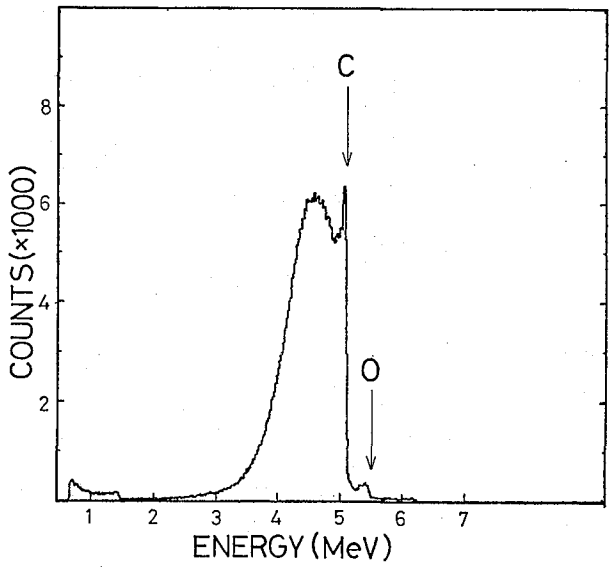

Fig. 11. 6.9 MeV proton backscattering spectrum observed at 150° from a cherry leaf.

means oxygen atoms take the place of carbon atoms just below the surface of the leaf. The greater part of oxygen atoms might be constituents of water molecules.

In the measurements mentioned previously, the bombardments were mostly carried out in a few minutes, and the yields of scattered particles obtained were enough to analyze elemental distributions. About the local distribution of light elements in the samples, the resolution of about 1 micron was obtained at the depth of 20 micron. In the measurement of ammonium citrate, the number of the molecules was about $5 \times 10^{16}/cm^2$. Judging from this result, it is possible to decide the elemental ratio of a sample of 10^{15} molecules/cm^2.

In conclusion the nuclear backscattering method using cyclotron can be used for the elemental analysis of organic matters of small amount and the determination of local distribution of light elements near the surface of a sample.

ACKNOWLEDGMENTS

The authors would like to express their thanks to Mr. K. Fujita, T. Miyanaga, N. Yamaguchi, and Miss. Y. Yokota for their assistance.

REFERENCES

(1) J. F. Ziegler, "New Uses of Ion Accelerators," Plenum, New York. (1975), pp. 73–158.
(2) P. D. Townsend, J. C. Kelly, and N. E. W. Hartley, "Ion Implantation, Sputtering and Their Applications," Academic Press, New York and London. (1976), pp. 181–198.
(3) H. Hiraki, *Hyomen (Surface)*, **14**, 330 (1976).
(4) C. F. Williamson, J. P. Boujot, and J. Picard "Tables of Range and Stopping Power of Chemical Elements for Charged Particles of Energy 0.05 to 500 MeV." Rapport CEA-R 3042, CENTRE D'ETUDES NUCLÉAIRES DE SACLAY. (1966).
(5) J. J. Ramirez *et al.*, *Phys. Rev.*, **179**, 310 (1969).
(6) G. Amsel *et al.*, *Nucl. Instr. & Meth.*, **92**, 481 (1971).